Magnetic field-driven lateral photovoltaic effect in the $Fe/SiO_2/p$-Si hybrid structure with the Schottky barrier

N.V. Volkov[a,b], M.V. Rautskii[a,*], A.S. Tarasov[a,c], I.A. Yakovlev[a], , I.A. Bondarev[a,c], A.V. Lukyanenko[a,c] S.N. Varnakov[a,b] and S.G. Ovchinnikov[a,b]

[a]Kirensky Institute of Physics, Federal Research Center KSC SB RAS, Krasnoyarsk, 660036 Russia
[b]Siberian State Aerospace University, Institute of Space Technology, Krasnoyarsk,660014 Russia
[c]Siberian Federal University, Institute of Engineering Physics and Radio Electronics, Krasnoyarsk, 660041 Russia
[*] E-mail address: rmv@iph.krasn.ru (M.V. Rautskii).

Abstract. We demonstrate that the lateral photovoltaic effect in the $Fe/SiO_2/p$-Si structure not only strongly depends on the optical radiation wavelength and temperature, but is also sensitive to external magnetic fields. The magnetic field lowers the absolute value of photovoltage regardless of the wavelength and temperature; however, the relative photovoltage variation significantly depends on these parameters. The lateral photovoltage is observed both on the Fe film and Si substrate sides and results from separation of photoinduced electrons and holes in a built-in electric field of the Schottky barrier with their subsequent diffusion to the structure in the lateral direction from the illuminated area. The observed features in the behavior of the lateral photovoltaic effect originate from the variation in the light absorption coefficient of the semiconductor and the related quantum efficiency upon light wavelength variation. In addition, an important role is played by the change in the characteristics of the Schottky barrier at the redistribution of optically generated carriers and temperature variation. The effect of the magnetic field is attributed to the Lorentz force, which bends trajectories of carriers drifting under the action of the Schottky barrier field and, consequently, suppresses the lateral photovoltaic effect.

1. Introduction

The lateral photovoltaic effect (LPE) was discovered by Walter Schottky as early as in 1930 [1]. With the beginning of tremendous upgrowth of semiconductor technology, it has been observed that the LPE manifests itself in many semiconductor systems and structures, including superlattices [2], heterostructures [3], two-dimensional electronic systems [4], and silicon Schottky barrier structures [5]. The search for novel LPE-based semiconductor devices with the required characteristics is currently being continued. This is dictated, first of all, by application tasks. The lateral photovoltage (LPV) was found to be strongly dependent on the light spot position with respect to electrodes, which allows fabricating position-sensitive detectors for sensing even minor displacements [6]. The range of application of such detectors is quite extensive and involves automatic control, positioning, surface profiling and other systems [7,8,9].

Surprisingly, the LPE appeared to be sensitive to external magnetic fields [10,11,12,13]. It is not excluded that the possibility of magnetic-field control of the LPV will open the way to fabrication of novel detectors and sensors or implementation of additional functionalities of the available devices. This property will make it possible, e.g., to fabricate magnetoresistive sensors sensitive to both the value and sign of a magnetic field [14,15] or double-control devices sensitive to both magnetic fields and optical radiation. Unfortunately, there has been a lack of studies on the effect of magnetic field on the LPE, so the mechanism of this effect still remains unclear.

Here, we report the results of investigations of the LPE behavior in the metal−insulator−semiconductor (MIS) hybrid structure $Fe/SiO_2/p$-Si with the Schottky barrier in external magnetic fields. Our attention is mainly focused upon the problems that have not been discussed yet, but can help advance understanding of the physical mechanisms of the influence of magnetic field on the LPE. These problems concern the features of the effect of magnetic field on the LPV in the $Fe/SiO_2/p$-Si

MIS hybrid structure with the Schottky barrier at different temperatures and optical radiation wavelengths.

2. Experimental

The technique for fabricating the $Fe/SiO_2/p$-Si structures was described by us in detail previously [16]. In this study, we used a 350 - μm-thick (100) p-Si wafer with a resistivity of 5 Ω·cm (a doping density of 2×10^{15} cm^{-3}) as a substrate. A 1.5-nm SiO_2 layer was deposited on the substrate's surface using the chemical method and a 5-nm iron layer was formed by thermal evaporation. All the processes were *in situ* monitored using high-energy electron backscatter diffraction (EBSD) and high-speed laser ellipsometry. The quality of layers and interfaces in the fabricated structures were characterized by cross-sectional transmission electron microscopy (TEM).

Samples for studying the LPE were (4.5×9.0)-mm^2 rectangles cut from the prepared structures (figure. 1). Two pairs of ohmic contacts about 0.5 mm in diameter were formed on the top of the Fe film and substrate backside to measure the LPV on the metal and semiconductor sides. The top contacts to the Fe film were formed from silver epoxy and the bottom contacts to the substrate were formed by alloying indium. None of the contacts showed any rectifying effects. Photovoltage was measured with a KEITHLEY-2182a nanovoltmeter.

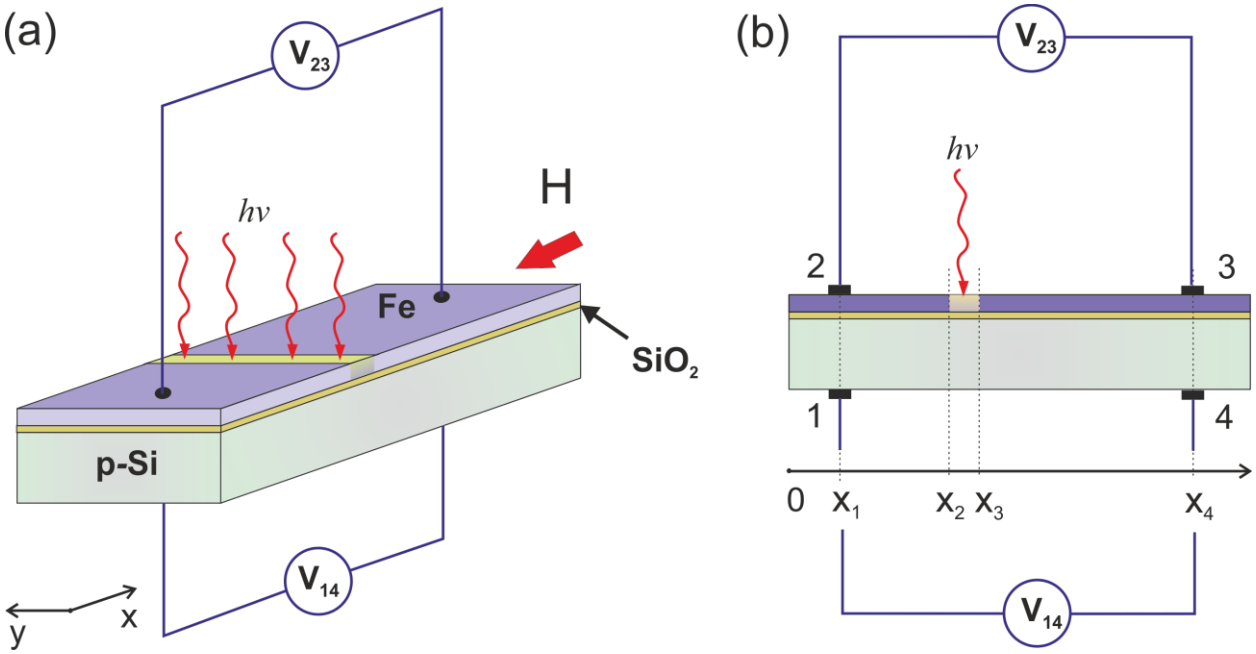

Figure 1. (a) Schematic of the sample for measuring the lateral photovoltage and measuring setup. (b) Coordinate system used to analyze the lateral photovoltaic effect.

The samples were irradiated from the metal film side by incandescent light transmitted through a prismatic monochromator. The light was focused in a narrow (0.5 mm) strip on the structure surface (figure 1). The narrow light beam position was fixed on the surface asymmetrically relative to the contacts for the entire measurement period. The light wavelength was tuned by the monochromator in the range from 0.4 to 1.4 μm. The radiation power density in each wavelength range was controlled by changing the incandescent lamp power. The average power density was ~40 mW/cm^2. During the measurements, the magnetic field was applied in the structure plane (figure 1a).

3. Results and discussion

3.1. LPE: Light wavelength dependence and effect of the magnetic field

First, let us discuss the dependence of the LPE on wavelength λ of the optical radiation inducing the effect and the spectral dependence of the LPE sensitivity to magnetic field *H*. Figure 2a shows the LPV dependences on λ for the $Fe/SiO_2/p$-Si structure, which were measured between contacts 1 and 4 on the Si side $V_{14}(\lambda)$ and between contacts 2 and 3 on the Fe side $V_{23}(\lambda)$. The contact configuration is shown in Figure 1. The measurements were performed at a temperature of 40 K without magnetic field and in a field of H=6 kOe. Here, we use the reduced LPV units $mV/(mW/cm^2)$ (the voltage induced by the incident light with unit power density). This is exclusively due to the experimental measurement conditions. The fact is that the power density of the optical radiation incident onto the structure after

passing the monochromator depends strongly enough on the wavelength to which the latter is tuned. As the experiments showed, in the investigated power range the LPV depended on the radiation power linearly with good accuracy.

The $V_{14}(\lambda)$ dependence has a pronounced peak in the wavelength range approximately from 0.8 to 1.1 μm with the maximum near 0.95 μm. The magnetic field decreases the intensity of the peak without its noticeable broadening or shift. The $V_{23}(\lambda)$ measurements using the pair of contacts on the Fe film side showed the dependence similar to $V_{14}(\lambda)$, but the voltages are lower by about two orders of magnitude and have the opposite sign (figure 2a). In addition, note that the peak in the $|V_{23}(\lambda)|$ dependence is narrower and lies approximately between 0.9 and 1.1 μm; its maximum is shifted toward larger wavelengths by 0.05 μm relative to the peak in the $V_{14}(\lambda)$ dependence. As in the measurements on the Si substrate side, the magnetic field lowers the intensity of the peak in the $|V_{23}(\lambda)|$ dependence without noticeable influence on its position and shape.

To thoroughly analyze the effect of magnetic field on the LPV, hereinafter referred to as the lateral photomagnetoelectric effect (LPMEE), we introduce its quantitative characteristic. We will use the quantity $MV = (V(H)-V(H=0))/V(H=0)$, which is analogous, to a certain extent, to the well-known magnetoresistance ratio. In our designations, the LPMEE ratio is MV_{14} for $V=V_{14}$ and MV_{23} for $V=V_{23}$.

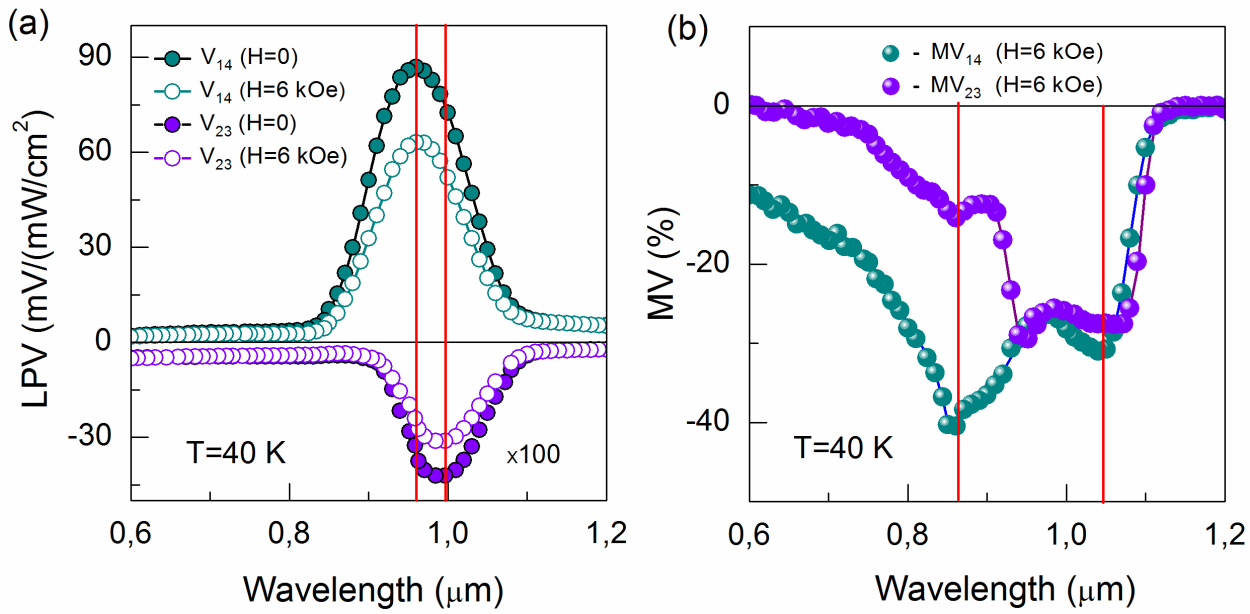

Figure 2. (a) Lateral photovoltage measured on the Si and Fe surfaces as a function of light wavelength ($V_{14}(\lambda)$ and $V_{23}(\lambda)$, respectively); the dependences are measured in fields of H=0 and H=6 kOe at T=40 K. For convenience, the $V_{23}(\lambda)$ dependences are multiplied by 100. (b) Lateral photomagnetoelectric effect ratio as a function of light wavelength on the Si and Fe surfaces ($MV_{14}(\lambda)$ and $MV_{23}(\lambda)$, respectively). H=6 kOe and T=40 K.

The $MV_{14}(\lambda)$ and $MV_{23}(\lambda)$ dependences obtained using the data from figure 2a are shown in figure 2b. The $|MV_{14}(\lambda)|$ dependence contains two pronounced peaks with the maxima at 0.85 and 1.05 μm. For the λ values smaller than 0.85 μm and larger than 1.05 μm, the LPMEE intensity drops, whereas in the λ range from 0.85 to 1.05 μm, the LPMVE ratio is fairly large and attains 40% in one of the maxima. Although the LPV measured on the Fe side is lower than that measured on the Si side by two orders of magnitude, the LPMEE ratios are comparable. At least, the $MV_{23}(\lambda)$ dependence at $\lambda > 0.95$ μm almost coincides with the $MV_{14}(\lambda)$ dependence, but at $\lambda < 0.95$ μm, the $|MV_{23}(\lambda)|$ dependence starts sharply decreasing, while the $|MV_{14}(\lambda)|$ dependence still continues rising.

3.2. LPE: Mechanism of the lateral photovoltage generation

The mechanism of the LPV generation in the structures with the Schottky barrier is illustrated in figure 3. The optical radiation absorbed in the p-Si substrate generates electron−hole pairs. The generated electrons and holes are instantaneously separated by a strong electric field in the depletion (space-charge) region. Electrons in the depletion region of the structure and within approximately diffusion length are swept into the Fe layer by the Schottky field, at the same time, holes are swept into the volume of the substrate. At irradiation of a local area of the substrate, such separation process result in creation of carrier density

gradient between the illuminated and non-illuminated zones. That forces the excess electrons in the metal and excess holes in the semiconductor to diffuse laterally from the illuminated zone.

Obviously, if the lateral distances from the electrodes in the illuminated area are different, the carrier densities at the electrodes are different, too. As a result, the potential difference (LPV) arises between the electrodes.

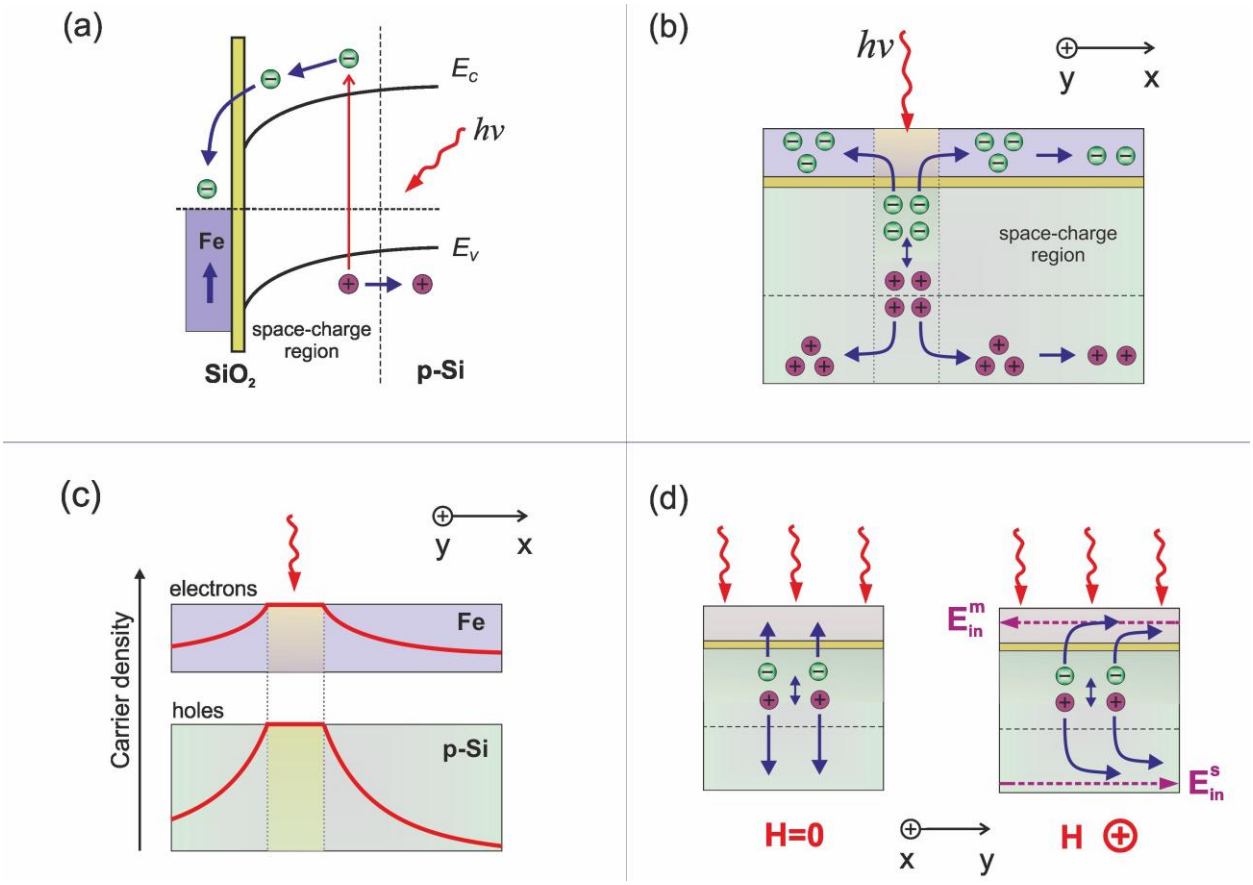

Figure 3. (a) Schematic energy band diagram of the MIS junction illustrating the electron−hole pair separation by the Schottky field. (b) The occurrence of the lateral photovoltage as a result of the electron−hole pair separation and lateral diffusion of carriers. (c) Schematic diagram of the stationary electron and hole density distributions on the Fe film and Si substrate surfaces. (d) The occurrence of the lateral photomagnetoelectric effect under the action of the Lorentz force which deflects carriers and thereby suppresses the lateral photovoltage.

According to the solution of the diffusion equation in the one-dimensional case, the electron and hole density distributions $n_m(x)$ and $p_s(x)$ in the metal and semiconductor, respectively, can be approximated by the Gaussian law

$$n_m(x) = n_i \exp\left(-\frac{x - x_i^{\,2}}{L_m^{\,2}}\right) \quad \text{and} \quad p_s(x) = p_i \exp\left(-\frac{x - x_i^{\,2}}{L_s^{\,2}}\right) \tag{1}$$

where, x_i is the position of the illuminated region boundary; n_i and p_i are the electron and hole densities at x_i, respectively; and L_m and L_s are the *effective* diffusion lengths for electrons in the metal and holes in the semiconductor, respectively. Carrier distributions (1) allow the potential distributions on the top of the Fe film $\phi_m(x)$ and Si substrate backside $\phi_s(x)$ to be determined. For simplicity, we solved the two-dimensional problem for both electrons in the Fe film and holes in the Si substrate, ignoring the interference of the electron and hole distributions under the assumption that the space-charge region shields this influence:

$$\varphi_m(x) = \frac{1}{4\pi\varepsilon_0\varepsilon}\int_S \frac{\rho_{em}(x')}{|\bar{r} - \bar{r}'|}dS' \quad \text{and} \quad \varphi_s(x) = \frac{1}{4\pi\varepsilon_0\varepsilon}\int_S \frac{\rho_{hs}(x')}{|\bar{r} - \bar{r}'|}dS' \tag{2}$$

where, $\rho_{em}(x)$ and $\rho_{hs}(x)$ are the charge densities produced by the distributions of electrons in Fe and holes in the bottom of the Si substrate, respectively. The integration is made over the entire structure surface S. The carrier distributions in the illuminated region of the structure are assumed to be homogeneous and change on either side of this region in accordance with equations (1). The V_{14} and V_{23} are the potential

differences between 1-4 and 2-3 contacts respectively: $V_{14} = \phi_s(x_1) - \phi_s(x_4)$ and $V_{14} = \phi_m(x_1) - \phi_m(x_4)$. Figure 4a presents the $\phi_s(x)$ and $\phi_m(x)$ dependences calculated using equations (2). The $V_{14}(\lambda)$ and $V_{23}(\lambda)$ behavior simulated in framework of the proposed model is shown in figure 4b.

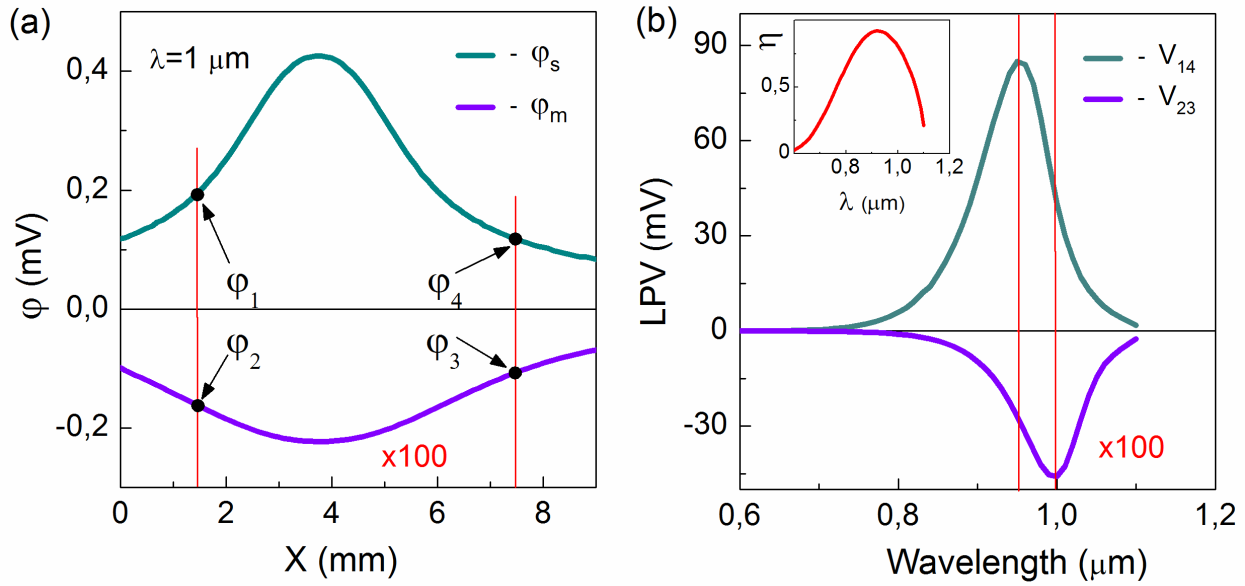

Figure 4. (a) Distribution of the optical radiation-induced electric potential on the Si substrate backside ϕ_s and in the Fe film ϕ_m. Arrows indicate the potentials in the contact positions. For convenience, $\phi_m(x)$ is multiplied by 100. (b) Simulated lateral photovoltage vs light wavelength on the Si substrate backside $V_{14}(\lambda)$ and in the Fe film $V_{23}\,\lambda$) (is multiplied by 100). Inset: quantum efficiency as a function of light wavelength.

The satisfactory agreement with the experiment was obtained only under quite a few assumptions. The carrier densities n_i and p_i in the illuminated region should be related not only to the radiation power, but also to the quantum efficiency $\eta(\lambda)$, which characterizes the efficiency of transformation of incident photons with different wavelengths to the photovoltage. From the long-wavelength side, $\eta(\lambda)$ has a cutoff at λ_c~1.12 μm, which is determined by the semiconductor band gap. In addition, the η value is decreased due to the small absorption coefficient α_s. In particular, due to small α_s the electron−hole pairs will be generated deep in the semiconductor, far from Schottky electric field which separates electrons and holes and, thus, prevents their fast recombination.

In the short-wavelength region, the fast drop of η is caused, on the contrary, by the large α_s value ($\geq 10^5$ cm^{-1}): the radiation is absorbed in the closest vicinity of the SiO_2/p-Si interface, where the electron−hole recombination times are small [17]. Certainly, the $n_i(\lambda)$and $p_i(\lambda)$dependences are affected also by the transmission and loss spectra for the metal film. However, they do not strongly influence the qualitative picture of the LPV behavior, since in the studied wavelength range the transparency of transition metal films with thicknesses smaller than 5 nm is relatively high (over 50%) and weakly dependent of the wavelength [18]. To simulate the $V_{14}(\lambda)$ and $V_{23}(\lambda)$ dependences, we used the $\eta(\lambda)$ dependence with the maximum at λ ~0.9μm (see inset in figure 4b), which is consistent with the experimental dependence for silicon-based Schottky diodes [17].

The different LPE signs obtained in the measurements from the Si and Fe sides can be easily explained: the potential difference in the semiconductor and metal is determined by the hole and electron density distribution, respectively. As for the large difference between the LPV values measured on the Si and Fe sides, its nature is questionable. The attempts to simulate this difference under the assumption of different L_m and L_s values made by Chongqi Yu and Hui Wang [5] did not yield a satisfactory result. The only way to obtain acceptable results is to assume the density of non-equilibrium electrons in the irradiated area of the metal to be much lower than the density of holes on the semiconductor substrate backside ($n_i << p_i$). To obtain the LPV values comparable with the experimental data, we should put $p_i = 10^{11}$ and $n_i = 0.06p_i$. Such a situation is feasible. In fact, under the action of the Schottky field, the electrons transited into the metal film lower the internal barrier potential inducing the reverse Schottky leakage current. This current consists of electrons reinjected to the semiconductor, which, being minority

carriers, hit the depletion region of the Schottky barrier and are instantaneously trapped at the reinjection point and therefore do not influence the hole potential distribution on the substrate backside.

The other necessary assumption concerns the behavior of the $L_m(\lambda)$ and $L_s(\lambda)$ dependences. To obtain the $V_{14}(\lambda)$ and $V_{23}(\lambda)$ dependences similar to those observed in the experiment, with the maxima in a certain spectral range, we should make a simple, yet not quite obvious assumption that electrons and holes with the larger rest energy of ($hc / \lambda - E_g$) have a longer *effective* diffusion length in the metal and semiconductor, respectively, [5]. This condition can be written as

$$L_m(\lambda) = L_m^0 + K_m (hc/\lambda - E_g)^{\beta} \quad \text{and} \quad L_s(\lambda) = L_s^0 + K_s (hc/\lambda - E_g)^{\beta} \qquad (3)$$

where, K_m and K_s are proportionality coefficients; β is the exponent; L_m^0 and L_s^0 are the respective diffusion lengths of electrons in the metal and holes in the semiconductor in the absence of the rest energy ($hc / \lambda = E_g$). The best agreement with the experiment was obtained at $K_m = K_s = 0.1$ and $\beta = 2$. The diffusion lengths used were $L_m^0 = 500$ μm and $L_s^0 = 50$ μm, which are consistent with the experiment. It should be emphasized that this difference between the diffusion lengths determines the positions of maxima in the $V_{14}(\lambda)$ and $|V_{23}(\lambda)|$ dependences.

3.3. LPE: Mechanism of the magnetic-field dependence

Let us now discuss possible mechanisms of the effect of magnetic field on the LPE. The relation of this effect to electron spin injection in the ferromagnetic metal and, consequently, reinjection from it seems improbable. In our opinion, it would be more realistic to assume the effect of magnetic field to be based on the Lorentz effect. Here, we should focus our attention on the experimental geometry, in which the direction of the magnetic field in the structure plane excludes its effect on the trajectories of charges moving laterally by means of diffusion. The effect of magnetic field can be related only with the transverse charge motion.

In our case, we observe, in fact, the analog of the photomagnetoelectric effect discovered by Kikoin and Noskov as early as in 1934 [19]. The effect consists in the occurrence of an electric field under irradiation of a strongly absorbing homogeneous semiconductor placed in a magnetic field. Photoinduced electrons and holes diffuse deep into the crystal. The diffusion current is deviated and split by the lateral magnetic field, which leads to the occurrence of a lateral electric field.

In our case, the lateral current in the structure with the Schottky barrier is related, first of all, to the drift motion of carriers under the action of the electric field in the space-charge region. Although the diffusion contribution also takes place in the structure regions where the electric field is missing. In addition, in contrast to the classical Kikoin−Noskov effect, electrons and holes move in different directions and are deviated to one side in the magnetic field (figure 3d), which leads to the occurrence of lateral electric fields with different signs in the upper and lower parts of the structure (E_{in}^m and E_{in}^s, respectively). Obviously, E_{in}^m and E_{in}^s will bend the carrier trajectories, which, in turn, will lead to a decrease in the photoinduced carrier density in the Fe film and on the backside substrate surface, and, in the long run, in the LPV, as was observed in the experiment. In our viewpoint, it is not time yet to build the quantitative LPMEE model in this work, since we should first clarify many items, including the nature of the spectral dependence of the effect (see Fig. 2d). Meanwhile, it is qualitatively clear that the spectral behavior is grounded on the strong dependence of α_s on λ and the related spectral dependence of $\eta(\lambda)$.

In terms of E_{in}^s, we have the following arguments concerning the effect of magnetic field on the LPE on the semiconductor substrate side. In the long-wavelength limit, the α_s and η values are small and the density of photogenerated holes in the space-charge region is low. These holes are accelerated in the Schottky field, acquire the higher drift velocity, and, consequently, are stronger affected by the lateral magnetic field. Thus, they make the main contribution to E_{in}^s. As the λ value is decreased, the α_s and η values grow, the increasing fraction of holes is generated in the space-charge region, and their contribution to the drift current increases, which leads to the occurrence of the diffusion component due to the generated carrier density gradient. As a result, the E_{in}^s value rapidly increases. In the short-wavelength limit, due to the large α_s value, almost all electron−hole pairs are generated in the space-charge region and can contribute to the drift and diffusion components of the lateral current. On the other

hand, in virtue of the above-discussed reasons, the η value drops rapidly, the generated electron−hole pair density sharply decreases, and, as a consequence, the E_{in}^{s} value strongly decreases.

The experimental spectral dependences MV_{14} are generally consistent with the above reasoning. The presence of the two above-mentioned maxima in $|MV_{14}(\lambda)|$ can apparently be explained by the competition between the drift and diffusion contributions and the induced lateral electric field. The above considerations can be expanded to the photoexcited electrons, which drift toward the iron film. Since the situation for electrons and holes in the Schottky structure is obviously asymmetric, the $MV_{23}(\lambda)$ behavior should be different from the $MV_{14}(\lambda)$ behavior, which is confirmed in figure 2b.

3.4. LPE: Temperature dependence

One more surprising result obtained by us is the LPE and LPMEE behavior upon temperature variation. Figure 5a shows the $V_{14}(\lambda)$ dependences obtained at different temperatures. It can be seen that, first, the effect value grows with a decrease in temperature from 40 to 30 K; after that, it starts decreasing, and then the peak in the $V_{14}(\lambda)$ dependence is inverted in the negative region; i.e., the LPV changes its sign with decreasing temperature. The LPMEE sign remains invariable; the absolute value of the LPV decreases in the magnetic field at all temperatures and wavelengths. Figure 5b shows the $MV_{14}(\lambda)$ dependences obtained at 30 and 10 K. At 40 and 30 K, the dependences are similar, except for a minor increase in the effect value in the latter case, whereas at 10 K the significant changes are observed. The effect value increased, the maximum in $|MV_{14}(\lambda)|$ shifted toward shorter wavelengths, and sharp jumps arose in the $MV_{14}(\lambda)$ curve at certain λ values. The occurrence of the jumps is explained by the fact that $V_{14}(\lambda)$ changes its sign at the point where $V_{14}(\lambda)$ turns to zero and $MV_{14}(\lambda)$ tends to infinity.

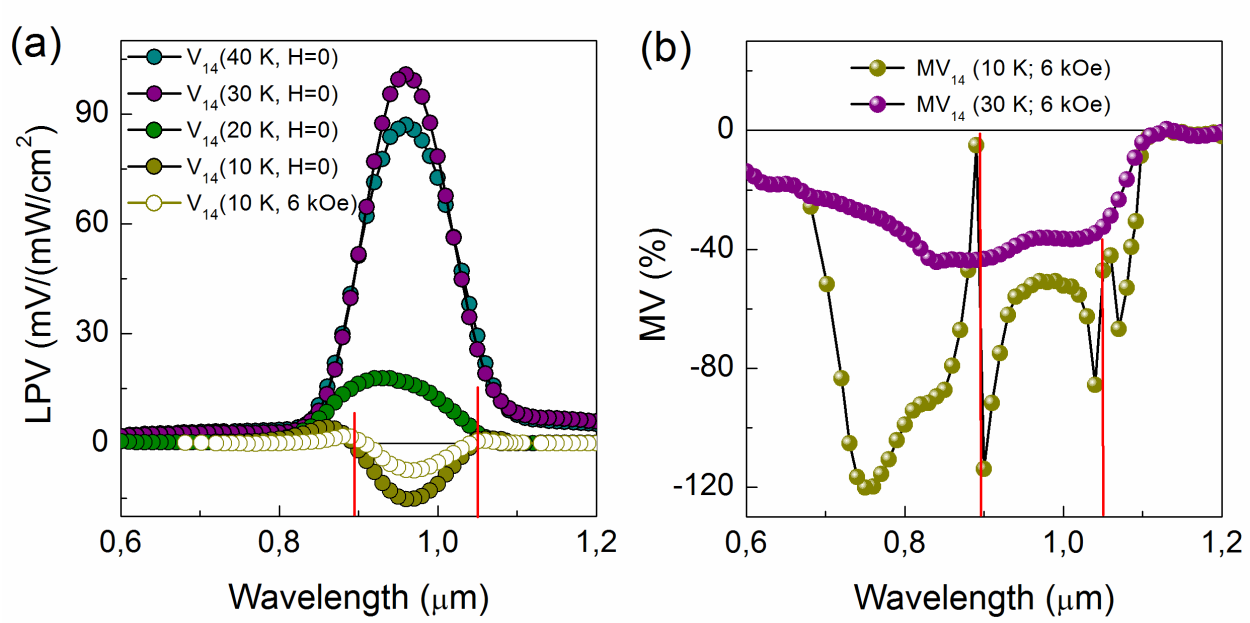

Figure 5. (a) Lateral photovoltage measured on the Si substrate backside as a function of light wavelength at different temperatures. At 10 K, the dependences obtained in fields of H=0 and H=6 kOe are shown. (b) Lateral photomagnetoelectric effect ratio as a function of light wavelength at temperatures of 10 and 30 K.

Figures 6a and 6b show temperature dependences of V_{14} (at H=0 and H=6 kOe) and MV_{14}, respectively, obtained at a fixed light wavelength of λ = 1 μm. It can be seen that the LPV maximum corresponds to a temperature of ~30 K; after that, the effect weakens, although non-monotonically, and changes its sign at approximately 16 K. Then, $|V_{14}(T)|$ rapidly acquires a relatively small value and stays almost constant with a further decrease in temperature. The LPMEE value first monotonically increases with a decrease in temperature, but at 22 K, the $|MV_{14}(T)|$ dependence has a pronounced maximum. The sharp jump in the $MV_{14}(T)$ dependence is caused, as for $MV_{14}(\lambda)$, by the fact that at this temperature $V_{14}(T)$ turns to zero.

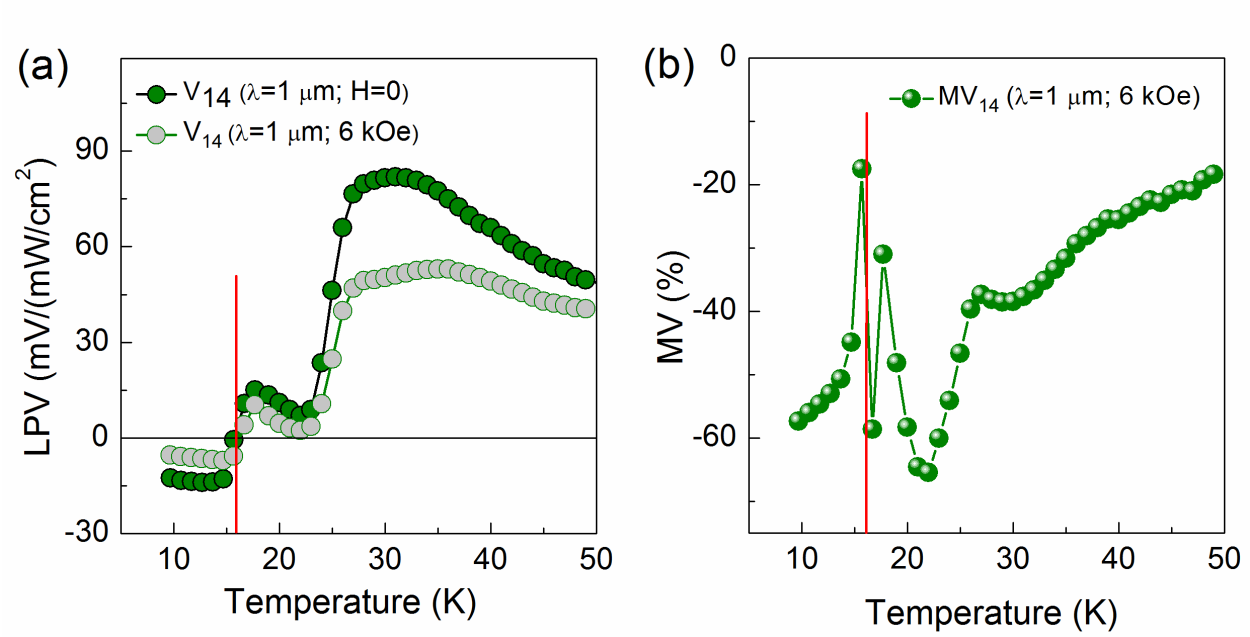

Figure 6. (a) Lateral photovoltage measured on the Si substrate backside as a function of temperature. The light wavelength is 1 μm. (b) Lateral photomagnetoelectric effect value as a function of temperature. The magnetic field is 6 kOe.

A decrease in the LPE value below ~30 K can be easily understood, while the change in the effect sign appeared surprising. Indeed, as the temperature is decreased, the acceptor levels in the *p*-type semiconductor start trapping holes, the number of majority carriers rapidly decreases, and the semiconductor becomes, in fact, intrinsic. The space charge region becomes smaller and, consequently, the Schottky field becomes weaker. The effect sign change can be indicative of the only thing: the potential difference between contacts on the Si side is now determined by electrons rather than holes. The following scenario is probably implemented: the strong decrease or even disappearance of the Schottky field enhances the diffusion contribution to the lateral current. The non-uniform distribution of photogenerated electron−hole pairs makes electrons and holes, which are not separated by the electric field of the junction any more, diffuse deep into the semiconductor. However, in virtue of different diffusivities of electrons and holes, the mobile carriers are spatially separated: electrons with the higher mobility pass deeper in the semiconductor than holes. Thus, electrons are accumulated near the lower substrate surface and then start diffusing in the lateral direction, inducing the LPV. The effect value will obviously be significantly smaller than at higher temperatures, when the drift contribution to the lateral current caused by the Schottky field works. This is what we observed in the experiment.

As for the LPMEE, it is still determined by the Lorentz force, which bends the trajectories of diffusing charges and thereby suppresses the LPE. The relative LPV variation in a magnetic field appears larger, despite the relatively small absolute value of V_{14}. Regarding the strongly non-monotonic $V_{14}(T)$ variation below T~30 K and the $MV_{14}(T)$ maximum at 22 K, they can be caused by the competition between the drift contribution, when the Schottky field separates photoexcited charges, and the diffusion contribution, which is related to the photoexcited carrier density gradient over the semiconductor depth, to the lateral current upon temperature variation.

4. Conclusion

Thus, we investigated the spectral and temperature dependences of the lateral photovoltaic effect and lateral photomagnetoelectric effect, which consists in the LPV variation in the Fe/SiO_2/p-Si structure in an applied magnetic field. The Schottky barrier plays a decisive role in the occurrence of both effects in the structure under study. The Schottky field separates optically generated electrons and holes in the lateral direction, which then laterally diffuse in the metal and semiconductor, respectively, contributing to the lateral photovoltaic effect. A decrease in the Schottky barrier at low temperatures leads, first, to a decrease in the lateral photovoltaic effect and, then, to the change of its sign. In the lateral photomagnetoelectric effect, the lateral electron and hole drift currents caused by the Schottky barrier field are deviated by a magnetic field; thus, the LPV decreases. The final behavior of the lateral

photovoltaic effect and lateral photomagnetoelectric effect is determined by the strong dependence of the interband absorption of the semiconductor and quantum efficiency on the optical radiation wavelength.

The disclosing of the lateral photomagnetoelectric effect promises broadening of functional capabilities of position-sensitive detectors based on the lateral photovoltaic effect. Magnetic field-controlled detectors or double-control sensors, which can be created on the basis of the new effect, will make it possible to simultaneously control the parameters of magnetic field and optical radiation. Finding optimal parameters of the structures for application requires further investigations. Taking into account the key role of the Schottky barrier in the lateral photovoltaic and photomagnetoelectric effects, it would be useful to experimentally investigate the structures with the topology suitable for bias-voltage control of the barrier parameters.

Acknowledgments

The reported study was funded by Russian Foundation for Basic Research, Government of Krasnoyarsk Territory, Krasnoyarsk Region Science and Technology Support Fund to the research project № 16-42-243046, and by Russian Foundation for Basic Research, project № 17-02-00302.

References

[1] Schottky W, Ueber den entstehungsort der photoelektronen in kupfer-kupferoxydul-photozellen, Phys. Z. 31 (1930) 913.

[2] B.F. Levine, R.H. Willens, C.G. Bethea, D. Brasen, Lateral photoeffect in thin amorphous superlattice films of Si and Ti grown on a Si substrate, Appl. Phys. Lett. 49 (1986) 1537–1539. doi:10.1063/1.97274.

[3] N. Tabatabaie, M.H. Meynadier, R.E. Nahory, J.P. Harbison, L.T. Florez, Large lateral photovoltaic effect in modulation-doped AlGaAs/GaAs heterostructures, Appl. Phys. Lett. 55 (1989) 792–794. doi:10.1063/1.101762.

[4] van Zalinge, B. Ozyilmaz, A. Böhm, R. van der Heijden, J.H. Wolter, P. Wyder, A. Bo, R.W. Van Der Heijden, J.H. Wolter, P. Wyder, H. Van Zalinge, Observation of the screening signature in the lateral photovoltage of electrons in the quantum Hall regime, Phys. Rev. B. 64 (2001) 235303. doi:10.1103/PhysRevB.64.235303.

[5] C. Yu, H. Wang, Large lateral photovoltaic effect in metal-(oxide-) semiconductor structures, Sensors (Switzerland). 10 (2010) 10155–10180. doi:10.3390/s101110155.

[6] H. Águas, L. Pereira, D. Costa, E. Fortunato, R. Martins, Linearity and sensitivity of MIS position sensitive detectors, J. Mater. Sci. 40 (2005) 1377–1381. doi:10.1007/s10853-005-0569-z.

[7] J. Contreras, C. Baptista, I. Ferreira, D. Costa, S. Pereira, H. Águas, E. Fortunato, R. Martins, R. Wierzbicki, H. Heerlein, Amorphous silicon position sensitive detectors applied to micropositioning, J. Non. Cryst. Solids. 352 (2006) 1792–1796. doi:10.1016/j.jnoncrysol.2006.02.026.

[8] A.J. Mäkynen, J.T. Kostamovaara, T.E. Rahkonen, CMOS Photodetectors for Industrial Position Sensing, IEEE Trans. Instrum. Meas. 43 (1994) 489–492. doi:10.1109/19.293476.

[9] A.J. Maekynen, H. Benten, T. Ruotsalainen, T.E. Rahkonen, J.T. Kostamovaara, CMOS position-sensitive photodetectors (PSDs) for integrated sensor systems, in: O. Loffeld (Ed.), 1997: pp. 89–100. doi:10.1117/12.287729.

[10] H. Wang, S.Q. Xiao, C.Q. Yu, Y.X. Xia, Q.Y. Jin, Z.H. Wang, Correlation of magnetoresistance and lateral photovoltage in Co 3Mn2O/SiO2/Si metal-oxide-semiconductor structure, New J. Phys. 10 (2008) 93006. doi:10.1088/1367-2630/10/9/093006.

[11] L.Z. Kong, H. Wang, S.Q. Xiao, J.J. Lu, Y.X. Xia, G.J. Hu, N. Dai, Z.H. Wang, Integrated properties of large lateral photovoltage and positive magnetoresistance in Co/Mn/Co/c-Si structures, J. Phys. D. Appl. Phys. 41 (2008) 52003. doi:10.1088/0022-3727/41/5/052003.

[12] Q. Zhang, J. Hu, D. Zheng, A. Dong and H. Wang, Magnetically tuned photoelectric response observed in nanoscale Co-SiO_2-Si structures, Nanotechnology 28 (2017). doi: : 10.1088/1361-6528/aa85ff.

[13] J. Hu, Q. Zhang, P. Zhou, C. Mei, X. Huang, A. Dong, D. Zheng, and H. Wang, Sensitive Photoelectric Response to Magnetic Field in p-Type Silicon-Based Structures, IEEE Photonics Technology Letters 29 (2017) 1848. doi: 10.1109/LPT.2017.2753405.

[14] N. V. Volkov, A.S. Tarasov, E. V. Eremin, F.A. Baron, S.N. Varnakov, S.G. Ovchinnikov, Extremely large magnetoresistance induced by optical irradiation in the Fe/SiO2/p-Si hybrid structure with Schottky barrier, J. Appl. Phys. 114 (2013) 93903. doi:10.1063/1.4819975.

[15] N. V Volkov, A.S. Tarasov, M. V Rautskii, A. V Lukyanenko, F.A. Baron, I.A. Bondarev, S.N. Varnakov, S.G. Ovchinnikov, The optically induced and bias-voltage-driven magnetoresistive effect in a silicon-based device, J. Surf. Investig. 9 (2015) 984–994. doi:10.1134/S1027451015050432.

[16] N. V. Volkov, A.S. Tarasov, E. V. Eremin, S.N. Varnakov, S.G. Ovchinnikov, S.M. Zharkov, Magnetic-field- and bias-sensitive conductivity of a hybrid Fe/SiO 2/p-Si structure in planar geometry, J. Appl. Phys. 109 (2011) 123924. doi:10.1063/1.3600056.

[17] K. Simon M. Sze, Physics of Semiconductor Devices, 3rd Edition, Wiley, New York, 2006.

[18] A. Axelevitch, B. Gorenstein, G. Golan, Investigation of Optical Transmission in Thin Metal Films, Phys. Procedia. 32 (2012) 1–13. doi:10.1016/j.phpro.2012.03.510.

[19] I. K. Kikoin and M. M. Noskov, A new photoelectric effect in cuprous oxide, Phys. Z. Sowjetunion. 5 (1934) 586–596.